Available online at www.sciencedirect.com

ScienceDirect

Procedia IUTAM 11 (2014) 3 – 14

Procedia IUTAM

www.elsevier.com/locate/procedia

Nonlinear Interfacial Wave Phenomena from the Micro- to the Macro-Scale

Coupled Ostrovsky equations for internal waves, with a background shear flow

A. Alias[a,b], R.H.J. Grimshaw[b], K.R. Khusnutdinova[b,*]

[a] *Department of Mathematics, University Malaysia Terengganu, 21030 Terengganu, Malaysia*
[b] *Department of Mathematical Sciences, Loughborough University, Loughborough LE11 3TU, UK*

Abstract

We study the behaviour of weakly nonlinear oceanic internal waves in the presence of background rotation and shear flow, when two distinct linear long wave modes have nearly coincident phase speeds. The waves are described by a system of coupled Ostrovsky equations, derived from the full set of Euler equations for incompressible density stratified fluid with a free surface and rigid bottom boundary conditions. We report here some preliminary results obtained when there is a background shear flow.

Selection and peer-review under responsibility of scientific committee of Nonlinear Interfacial Wave Phenomena from the Micro- to the Macro-Scale

Keywords: Internal waves; Earth's rotation; shear flow; strong interaction

1. Introduction

The Korteweg - de Vries (KdV) and Ostrovsky equations are the canonical models for the description of internal solitary waves and their relatives, commonly observed in the oceans (for example, see the reviews [1,2,3] and references therein). Both equations are derived on the assumption that the dynamics is dominated only by a single linear long wave mode and written in a reference frame moving with the linear long wave speed. The Ostrovsky equation [4,5,6]

$$\{A_t + \nu A A_x + \lambda A_{xxx}\}_x = \gamma A \tag{1}$$

is an extension of the KdV equation

$$A_t + \nu A A_x + \lambda A_{xxx} = 0 \tag{2}$$

in the presence of background rotation. In these equations, $A(x,t)$ is the amplitude of the linear long wave mode $\phi(z)$ corresponding to the linear long wave phase speed c, which is determined from the modal equations

$$(\rho_0 W^2 \phi_z)_z + \rho_0 N^2 \phi = 0\,, \tag{3}$$

$$\phi = 0 \quad \text{at} \quad z = -h\,, \quad \text{and} \quad W^2\phi_z = g\phi \quad \text{at} \quad z = 0\,. \tag{4}$$

* Corresponding author. Tel.: +44-1509-228202 ; fax: +44-1509-223969.
E-mail address: K.Khusnutdinova@lboro.ac.uk

Selection and peer-review under responsibility of scientific committee of Nonlinear Interfacial Wave Phenomena from the Micro- to the Macro-Scale
doi:10.1016/j.piutam.2014.01.043

Here $\rho_0(z)$ is the stable background density stratification, $\rho_0 N^2 = -g\rho_{0z}$, $W = c - u_0$ where $u_0(z)$ is the background shear flow, and it is assumed there are no critical levels, that is $W \neq 0$ for any z in the flow domain. Equations (1, 2) are expressed in a reference frame moving with the speed c. The coefficients in these equations are given by

$$I\nu = 3\int_{-h}^{0} \rho_0 W^2 \phi_z^3\, dz\,, \quad I\lambda = \int_{-h}^{0} \rho_0 W^2 \phi^2\, dz\,, \quad I\gamma = f^2 \int_{-h}^{0} \rho_0 \Phi \phi_z\, dz\,, \tag{5}$$

where

$$I = 2\int_{-h}^{0} \rho_0 W \phi_z^2\, dz\,, \quad \rho_0 W\Phi = \rho_0 W\phi_z - (\rho_0 u_0)_z \phi\,, \tag{6}$$

and f is the Coriolis parameter. Note that when there is no shear flow, that is $u_0(z) \equiv 0$, then $\Phi \equiv \phi_z$ and $\gamma = f^2/2c$.

The effect of the Earth's rotation for the time evolution of an internal wave becomes important when the wave propagates for several inertial periods. For oceanic internal waves $\lambda\gamma > 0$, and then it is known that equation (1) does not support steady solitary wave solutions, see [7] and the references therein. Recently, it was established that the long-time effect of rotation is the destruction of the initial internal solitary wave by the radiation of small-amplitude inertia-gravity waves, and the emergence of a propagating nonlinear wave packet [7,8,9,10]. It is worth noting that the same phenomenon was observed independently in [11] in the context of waves in solids. Indeed, the discrete model in [11] can be related to the two-directional generalisation of the Ostrovsky equation derived in [12].

It is known that for internal waves it is possible for the phase speeds of different modes to be nearly coincident, and then there will be a resonant transfer of energy between the waves [13]. In this case, the KdV equation is replaced by two coupled KdV equations, describing a strong interaction between internal solitary waves of different modes, see [14,15]. Various families of solitary waves are supported by coupled KdV equations depending on the structure of the linear dispersion relation: pure solitary waves, generalised solitary waves and envelope solitary waves , see the review [15]. In [16] we extended the derivation of the coupled KdV equations to take account of background rotation, and also a background shear flow. We found that then the single Ostrovsky equation (1) is replaced by two coupled Ostrovsky equations, each equation having both linear and nonlinear coupling terms. Coupled Ostrovsky equations were also derived in the context of waves in layered elastic waveguides [17,18]. Thus, this model belongs to the class of canonical mathematical models of nonlinear wave theory, inviting a detailed study of the dynamics of its solutions.

The paper is organised as follows. In section 2.1 we briefly overview the derivation of a pair of coupled Ostrovsky equations from the complete set of Euler equations for an inviscid, incompressible, density stratified fluid with boundary conditions appropriate to an oceanic situation, using the asymptotic multiple-scales expansions. The effect of background shear is investigated using a three-layer model in section 2.2. In section 3 we analyse the linear dispersion relation. In section 4, based on the analysis of the previous section, we present some preliminary numerical simulations using a pseudo-spectral method. We show that a shear flow allows for a configuration when initial solitary-like waves in the coupled system are destroyed, and replaced by nonlinear envelope wave packets, a two-component counterpart of the outcome for the single Ostrovsky equation (1), previously studied for the coupled system in the absence of the shear flow in [16]. Our preliminary analysis shows that this is not the only scenario possible when a shear flow is present, and invites further studies.

2. Coupled Ostrovsky equations

2.1. Derivation

Let us consider two-dimensional flow of an inviscid, incompressible fluid on an f-plane. In the basic state the fluid has a density stratification $\rho_0(z)$, a corresponding pressure $p_0(z)$ such that $p_{0z} = -g\rho_0$ and a horizontal shear flow $u_0(z)$ in the x-direction. When $u_0 \neq 0$, this basic state is maintained by a body force. Then the equations of motion relative

to this basic state are given by

$$\rho_0(u_t + u_0u_x + wu_{0z}) + p_x = -(\rho_0 + \rho)(uu_x + wu_z - fv) - \rho(u_t + u_0u_x + wu_{0z}), \tag{7}$$
$$\rho_0(v_t + u_0v_x + fu) + \rho f u_0 = -(\rho_0 + \rho)(uv_x + wv_z) - \rho(v_t + u_0v_x) - \rho f u, \tag{8}$$
$$p_z + g\rho = -(\rho_0 + \rho)(w_t + (u_0 + u)w_x + ww_z), \tag{9}$$
$$g(\rho_t + u_0\rho_x) - \rho_0 N^2 w = -g(u\rho_x + w\rho_z), \tag{10}$$
$$u_x + w_z = 0. \tag{11}$$

Here, the terms $(u_0 + u, v, w)$ are the velocity components in the (x, y, z) directions, $\rho_0 + \rho$ is the density, $p_0 + p$ is the pressure, t is time, $N(z)$ is the buoyancy frequency, defined by $\rho_0 N^2 = -g\rho_{0z}$ and f is the Coriolis frequency. The free surface and rigid bottom boundary conditions to the above problem are given by

$$p_0 + p = 0 \qquad \text{at} \qquad z = \eta, \tag{12}$$
$$\eta_t + (u_0 + u)\eta_x = w \qquad \text{at} \qquad z = \eta, \tag{13}$$
$$w = 0 \qquad \text{at} \qquad z = -h. \tag{14}$$

The constant h denotes the undisturbed depth of the fluid, and the function η denotes the displacement of the free surface from its undisturbed position $z = 0$. In our derivation, we use a new variable ζ as the vertical particle displacement which is related to the vertical speed, w. It is defined by the equation

$$\zeta_t + (u_0 + u)\zeta_x + w\zeta_z = w, \tag{15}$$

and satisfies the boundary condition

$$\zeta = \eta \qquad \text{at} \qquad z = \eta. \tag{16}$$

The system of coupled Ostrovsky equations is derived using the Eulerian formulation, following a similar strategy to the derivation of coupled KdV equations using the Lagrangian formulation in [14,15]. A full account is described in [16]. At the leading linear long wave order, and in the absence of any rotation, the solution for ζ is given by an expression of the form $A(x - ct)\phi(z)$ where the modal function is given by (3), (4). In general there is an infinite set of solutions for $[\phi(z), c]$. Here we consider the case when there are two modes with nearly coincident speeds $c_1 = c$ and $c_2 = c + \epsilon^2\Delta$, $\epsilon \ll 1$, where Δ is the detuning parameter. Importantly, we assume that the modal functions $\phi_1(z), \phi_2(z)$ are *distinct*, and each satisfy the system (3), (4), that is

$$(\rho_0 W_i^2 \phi_{iz})_z + \rho_0 N^2 \phi_i = 0, \quad i = 1, 2 \tag{17}$$
$$\phi_i = 0 \quad \text{at} \quad z = -h, \quad \text{and} \quad W_i^2 \phi_{iz} = g\phi_i \quad \text{at} \quad z = 0. \tag{18}$$

Here $W_i = c_i - u_0(z)$ where c_i is the long wave speed corresponding to the mode $\phi_i(z)$, $i = 1, 2$. The two modal systems (17), (18) imply that

$$\int_{-h}^{0} \rho_0 (W_1^2 - W_2^2)\phi_{1z}\phi_{2z} dz = 0. \tag{19}$$

Since in general $W_1 - W_2 = c_1 - c_2 \neq 0$, it follows that the two modes satisfy an orthogonality condition,

$$\int_{-h}^{0} \rho_0 [c_1 + c_2 - 2u_0]\phi_{1z}\phi_{2z}\, dz = 0, \quad \text{so that} \quad \int_{-h}^{0} \rho_0 W \phi_{1z}\phi_{2z}\, dz \approx 0. \tag{20}$$

Here, and in the sequel, $W_i = W = c - u_0(z)$ with an error of order ϵ^2.

Next we introduce the scaled variables

$$\tau = \epsilon\alpha t, \quad s = \epsilon(x - ct), \quad f = \alpha\tilde{f} \tag{21}$$

where $\alpha = \epsilon^2$ and seek a solution in the form of asymptotic multiple - scales expansions

$$(\zeta, u, \rho, p) = \alpha(\zeta_1, u_1, \rho_1, p_1) + \alpha^2(\zeta_2, u_2, \rho_2, p_2) + \cdots, \tag{22}$$
$$(w, v) = \alpha\epsilon(w_1, v_1) + \alpha^2\epsilon(w_2, v_2) + \cdots. \tag{23}$$

Substituting these expansions into the system (7) - (11), and assuming that two waves A_1 and A_2 are present at the leading order, we obtain

$$\zeta_1 = A_1(s,\tau)\phi_1(z) + A_2(s,\tau)\phi_2(z)\,, \tag{24}$$
$$u_1 = A_1\{W\phi_1\}_z + A_2\{W\phi_2\}_z\,, \tag{25}$$
$$w_1 = -A_{1s}W\phi_1 - A_{2s}W\phi_2\,, \tag{26}$$
$$p_1 = \rho_0 A_1 W^2\phi_{1z} + \rho_0 A_2 W^2\phi_{2z}\,, \tag{27}$$
$$g\rho_1 = \rho_0 N^2\zeta_1\,, \tag{28}$$
$$v_1 = \tilde{f}(B_1\Phi_1 + B_2\Phi_2)\,, \quad \rho_0 W\Phi_{1,2} = \rho_0 W\phi_{1z,2z} - (\rho_0 u_0)_z\phi_{1,2}\,, \quad B_{1s,2s} = A_{1,2}\,. \tag{29}$$

Importantly, the exact solution of the linearised equations should contain the exact expressions W_1 and W_2 in the terms related to the first and second waves, respectively, rather than just W. In fact, $W_1 = W$ through our choice of $c_1 = c$, but there is an $O(\epsilon^2)$ difference between W_2 and W since $c_2 = c + \epsilon^2\Delta$. This difference between the exact and leading order solutions necessitates the introduction of correction terms at the next order, in order to recover the distinct modal equations for the functions ϕ_1 and ϕ_2.

Collecting terms of the second order for each equation, and calculating the correction terms originating from the leading order, the following set of equations are obtained,

$$\rho_0(-Wu_{2s} + u_{0z}w_2) + p_{2s} = -\rho_0(u_{1\tau} + u_1u_{1s} + w_1u_{1z}) + \rho_1(Wu_{1s} - u_{0z}w_1) + \rho_0\tilde{f}v_1, \tag{30}$$
$$\rho_0(\tilde{f}u_2 - Wv_{2s}) + \rho_2\tilde{f}u_0 = -\rho_0(v_{1\tau} + u_1v_{1s} + w_1v_{1z}) + \rho_1 Wv_{1s} - \rho_1\tilde{f}u_1\,, \tag{31}$$
$$p_{2z} + g\rho_2 = \rho_0 Ww_{1s} + 2\Delta A_2\{\rho_0 W\phi_{2z}\}_z\,, \tag{32}$$
$$-gW\rho_{2s} - \rho_0 N^2 w_2 = -g(\rho_{1\tau} + u_1\rho_{1s} + w_1\rho_{1z})\,, \tag{33}$$
$$u_{2s} + w_{2z} = 0\,, \tag{34}$$
$$W\zeta_{2s} + w_2 = \zeta_{1\tau} + u_1\zeta_{1s} + w_1\zeta_{1z}\,. \tag{35}$$

Here, the extra term proportional to A_2 in (32) comes from the afore-mentioned difference between W_2 and W in the leading order pressure term (27) creating in effect a contribution to p_1, but there is no analogous term in (30) as there is a cancellation between the corrections to u_1 and p_1. Similarly, the boundary conditions (14) - (13), (16) yield

$$w_2 = 0 \quad \text{at} \quad z = -h\,, \tag{36}$$
$$p_2 - \rho_0 g\eta_2 + p_{1z}\eta_1 - \frac{1}{2}\rho_{0z}g\eta_1^2 - 2\Delta\rho_0 W\phi_{2z}A_2 = 0 \quad \text{at} \quad z = 0\,, \tag{37}$$
$$w_2 + w_{1z}\eta_1 - \eta_{1\tau} + W\eta_{2s} - u_{0z}\eta_1\eta_{1s} - u_1\eta_{1s} = 0 \quad \text{at} \quad z = 0\,, \tag{38}$$
$$\zeta_2 + \zeta_{1z}\eta_1 - \eta_2 = 0 \quad \text{at} \quad z = 0\,. \tag{39}$$

Eliminating all variables in favour of ζ_2 yields

$$\{\rho_0 W^2\zeta_{2sz}\}_z + \rho_0 N^2\zeta_{2s} = M_2 \quad \text{at} \quad -h < z < 0\,, \tag{40}$$
$$\zeta_2 = 0 \quad \text{at} \quad z = -h\,, \quad \rho_0 W^2\zeta_{2sz} - \rho_0 g\zeta_{2s} = N_2 \quad \text{at} \quad z = 0\,, \tag{41}$$

where M_2, N_2 are known expressions containing terms in A_i and their derivatives. The full expressions can be found in [16].

Two compatibility conditions need to be imposed on the system (40), (41), given by

$$\int_{-h}^{0} M_2\phi_{1,2}\,dz - [N_2\phi_{1,2}]_{z=0} = 0\,, \tag{42}$$

where $\phi_{1,2}$ are evaluated at the leading order. These compatibility conditions lead to the coupled Ostrovsky equations

$$I_1(A_{1\tau} + \mu_1 A_1A_{1s} + \lambda_1 A_{1sss} - \gamma_1 B_1) + \nu_1[A_1A_2]_s + \nu_2 A_2A_{2s} + \lambda_{12}A_{2sss} - \gamma_{12}B_2 = 0\,, \tag{43}$$
$$I_2(A_{2\tau} + \mu_2 A_2A_{2s} + \lambda_2 A_{2sss} + \Delta A_{2s} - \gamma_2 B_2) + \nu_2[A_1A_2]_s + \nu_1 A_1A_{1s} + \lambda_{21}A_{1sss} - \gamma_{21}B_1 = 0\,, \tag{44}$$

where $B_{1s} = A_1, B_{2s} = A_2$, and the coefficients are given by

$$I_i\mu_i = 3\int_{-h}^{0} \rho_0(c-u_0)^2\phi_{iz}^3\,dz\,, \tag{45}$$

$$I_i\lambda_i = \int_{-h}^{0} \rho_0(c-u_0)^2{\phi_i}^2\,dz\,, \tag{46}$$

$$I_i = 2\int_{-h}^{0} \rho_0(c-u_0)\phi_{iz}^2\,dz\,, \tag{47}$$

$$\lambda_{12} = \lambda_{21} = \int_{-h}^{0} \rho_0(c-u_0)^2\phi_1\phi_2\,dz\,, \tag{48}$$

$$\nu_1 = 3\int_{-h}^{0} \rho_0(c-u_0)^2\phi_{1z}^2\phi_{2z}\,dz\,, \tag{49}$$

$$\nu_2 = 3\int_{-h}^{0} \rho_0(c-u_0)^2\phi_{2z}^2\phi_{1z}\,dz\,, \tag{50}$$

$$I_i\gamma_i = \tilde{f}^2\int_{-h}^{0} \rho_0\Phi_i\phi_{iz}\,dz\,, \tag{51}$$

$$\gamma_{ij} = \tilde{f}^2\int_{-h}^{0} \rho_0\Phi_i\phi_{jz}\,dz\,. \tag{52}$$

Here $i, j = 1, 2$. If there is no shear flow, that is $u_0 = 0$, then $\gamma_1 = \gamma_2 = \tilde{f}^2/2c$ and $\gamma_{12} = \gamma_{21} = 0$.

We scale the dependent and independent variables as

$$A_1 = \frac{u}{\mu_1}\,, \quad A_2 = \frac{v}{\mu_2}\,, \quad s = \lambda_1^{1/2}X\,, \quad \tau = \lambda_1^{1/2}T\,, \tag{53}$$

assuming that $\lambda_1 > 0, \mu_{1,2} \neq 0$ without loss of generality. Then equations (43), (44) become

$$(u_T + uu_X + u_{XXX} + n(uv)_X + mvv_X + \alpha v_{XXX})_X = \beta u + \gamma v, \tag{54}$$

$$(v_T + vv_X + \delta v_{XXX} + \Delta v_X + p(uv)_X + quu_X + \lambda u_{XXX})_X = \mu v + \nu u, \tag{55}$$

where

$$n = \frac{\nu_1}{I_1\mu_2}, \quad m = \frac{\mu_1\nu_2}{I_1\mu_2^2}, \quad \alpha = \frac{\lambda_{12}\mu_1}{\lambda_1 I_1\mu_2}, \quad \beta = \gamma_1\lambda_1, \quad \gamma = \frac{\gamma_{12}\mu_1\lambda_1}{I_1\mu_2},$$
$$\delta = \frac{\lambda_2}{\lambda_1}, \quad p = \frac{\nu_2}{I_2\mu_1}, \quad q = \frac{\mu_2\nu_1}{I_2\mu_1^2}, \quad \lambda = \frac{\lambda_{21}\mu_2}{\lambda_1 I_2\mu_1}, \quad \mu = \gamma_2\lambda_1, \quad \nu = \frac{\gamma_{21}\mu_2\lambda_1}{I_2\mu_1}. \tag{56}$$

Here,

$$\frac{q}{n} = \frac{p}{m} = \frac{\lambda}{\alpha} = \frac{\gamma_{12}\nu}{\gamma_{21}\gamma} = \frac{I_1\mu_2^2}{I_2\mu_1^2}\,, \quad \frac{\alpha\lambda}{\delta} = \frac{\lambda_{12}^2}{\lambda_1\lambda_2 I_1 I_2} < 1\,. \tag{57}$$

Note that the scaled variables u and v, and the coefficient p should not be confused with the velocity components and the pressure, which are not used any more.

2.2. Three-layer flow with a piecewise-constant current

As a simple example of the effect of background shear, we consider the three-layer fluid, $-h < z < 0$, with interfaces at $z = -h_2 - h_1, z = -h_1$, where $h = h_1 + h_2 + h_3$. The background density is

$$\rho_0(z) = \rho_3 + (\rho_2 - \rho_3)H(z + h_2 + h_1) + (\rho_1 - \rho_2)H(z + h_1)\,,$$

and we assume that there is also a piecewise constant current,

$$u_0(z) = U_3 + (U_2 - U_3)H(z + h_2 + h_1) + (U_1 - U_2)H(z + h_1)\,,$$

which we view as an approximation to an actual smooth current profile. Here, $H(\dots)$ is the Heaviside function, and without loss of generality, we can set $U_2 = 0$. We consider only internal waves, and impose rigid boundaries at $z = -h, 0$. The modal function can now be readily calculated. Omitting details, we find that a resonance with two distinct linear modes occurs in the asymptotic limit $h_2 >> h_1, h_3$, and is expressed by

$$c = U_1 \pm \{\frac{gh_1(\rho_2 - \rho_1)}{\rho_1}\}^{1/2} = U_3 \pm \{\frac{gh_3(\rho_3 - \rho_2)}{\rho_3}\}^{1/2}. \tag{58}$$

For given densities $\rho_{1,2,3}$ and layer depths $h_{1,3}$, these conditions determine the currents U_1, U_3.

All coefficients in the coupled Ostrovsky equation can now be calculated,

$$I_1\mu_1 = -\frac{3\rho_1(c-U_1)^2}{h_1^2}, \quad I_2\mu_2 = \frac{3\rho_3(c-U_3)^2}{h_3^2}, \tag{59}$$

$$I_1\lambda_1 = I_2\lambda_2 = \frac{c^2\rho_2 h_2}{3}, \tag{60}$$

$$I_1 = \frac{2\rho_1(c-U_1)}{h_1}, \quad I_2 = \frac{2\rho_3(c-U_3)}{h_3}, \tag{61}$$

$$\lambda_{12} = \lambda_{21} = \frac{c^2\rho_2\, h_2}{6}, \tag{62}$$

$$\nu_1 = \nu_2 = 0. \tag{63}$$

In order to find the coefficients $\gamma_{1,2,12}$ we must evaluate $\Phi_{1,2}$, where

$$\Phi_{1,2} = \phi_{1z,2z} - \frac{(\rho_0 u_0)_z}{\rho_0 W}\phi_{1,2}. \tag{64}$$

Here $\rho, W = c - u_0$ are piecewise constant, so the second term behaves like a δ-function. When the δ-function multiplies a function $f(x)$ having a jump discontinuity at $x = 0$, as here, we use the expression,

$$\int_a^b f(x)\delta(x)dx = \frac{1}{2}[f(0+) + f(0-)], \tag{65}$$

for any interval $[a, b]$ containing $x = 0$. We then find that

$$I_1\gamma_1 = \frac{\rho_1\tilde{f}^2}{h_1}\{1 + \frac{1}{2}\log[\frac{|W_2|}{|W_1|}] - \frac{U_1}{2W_1}\log[\frac{\rho_2}{\rho_1}]\}, \tag{66}$$

$$I_2\gamma_2 = \frac{\rho_3\tilde{f}^2}{h_3}\{1 + \frac{1}{2}\log[\frac{|W_2|}{|W_3|}] - \frac{U_3}{2W_3}\log[\frac{\rho_2}{\rho_3}]\}, \tag{67}$$

$$\gamma_{12} = \gamma_{21} = 0. \tag{68}$$

We let $g_1 = g(\rho_2 - \rho_1)/\rho_1$, $g_3 = g(\rho_3 - \rho_2)/\rho_3$ and use the Boussinesq approximation that otherwise $\rho_1 \approx \rho_2 \approx \rho_3$. We then obtain

$$n = m = p = q = \gamma = \nu = 0, \tag{69}$$

$$\delta = \frac{h_3(c-U_1)}{h_1(c-U_3)} = -2\alpha, \quad \lambda = -\frac{1}{2}, \tag{70}$$

$$\beta = \frac{c^2h_1h_2\rho_2\tilde{f}^2[1 + \frac{1}{2}\log|c/(c-U_1)|]}{12\rho_1(c-U_1)^2}, \tag{71}$$

$$\mu = \frac{c^2h_1h_2\rho_2\tilde{f}^2[1 + \frac{1}{2}\log|c/(c-U_3)|]}{12\rho_1(c-U_1)(c-U_3)}, \tag{72}$$

$$\tag{73}$$

so that

$$\mu = \beta F, \quad F = \left(\frac{c-U_1}{c-U_3}\right)\frac{1 + \frac{1}{2}\log|c/(c-U_3)|}{1 + \frac{1}{2}\log|c/(c-U_1)|}. \tag{74}$$

There are four possibilities according to the choices of the signs for the value of c in (58). To avoid a critical layer, we choose

$$c > \max[U_1, 0, U_3]\,,$$

where we recall that we have set $U_2 = 0$. This condition then implies that $c = U_1 + \sqrt{g_1 h_1} = U_3 + \sqrt{g_3 h_3}$, and in the remainder of this paper we restrict our considerations to this case. Explicitly evaluating the coefficients in (54), (55), we obtain

$$\delta = \sqrt{\frac{g_1 h_3}{g_3 h_1}} = -2\alpha\,, \quad \lambda = -\frac{1}{2}\,, \tag{75}$$

$$\beta = \frac{h_2 \tilde{f}^2 (\sqrt{g_1 h_1} + U_1)^2 [1 + \frac{1}{2}\log|\sqrt{g_1 h_1} + U_1|/\sqrt{g_1 h_1}]]}{12 g_1}\,, \tag{76}$$

$$\mu = \beta F\,, \quad F = \sqrt{\frac{g_1 h_1}{g_3 h_3}}\,\frac{[1 + \frac{1}{2}\log|\sqrt{g_3 h_3} + U_3|/\sqrt{g_3 h_3}]}{[1 + \frac{1}{2}\log|\sqrt{g_1 h_1} + U_1|/\sqrt{g_1 h_1}]}\,. \tag{77}$$

Note that $\tilde{f}, h_2$ are independent free parameters, so that we may choose $|\beta| = 1\, m^2 s^{-2}$, and also allow Δ to be a free available parameter. But then μ is determined by the factor F, which depends on $g_{1,3}, h_{1,3}, U_{1,3}$.

3. Linear dispersion relation

The linear dispersion relation is obtained by seeking solutions of the linearised equations in the form

$$u = u_0 e^{ik(X - c_p T)} + c.c., \quad v = v_0 e^{ik(X - c_p T)} + c.c.\,, \tag{78}$$

where k is the wavenumber and c_p is the phase speed. This leads to the equations

$$(c_p - C_1(k))u_0 + (\alpha k^2 - \frac{\gamma}{k^2})v_0 = 0\,, \tag{79}$$

$$(\lambda k^2 - \frac{\nu}{k^2})u_0 + (c_p - C_2(k))v_0 = 0\,, \tag{80}$$

where

$$C_1(k) = -k^2 + \frac{\beta}{k^2}\,, \quad C_2(k) = \Delta - \delta k^2 + \frac{\mu}{k^2}\,. \tag{81}$$

The determinant of this 2×2 system yields the dispersion relation

$$(c_p - C_1(k))(c_p - C_2(k)) = D(k) = (\alpha k^2 - \frac{\gamma}{k^2})(\lambda k^2 - \frac{\nu}{k^2})\,. \tag{82}$$

Solving this dispersion relation we obtain the two branches of the dispersion relation,

$$c_p = c_{p1,p2} = \frac{C_1 + C_2}{2} \pm \frac{1}{2}\{4D + (C_1 - C_2)^2\}^{1/2}\,. \tag{83}$$

Here $C_{1,2}(k)$ are the linear phase speeds of the uncoupled Ostrovsky equations, obtained formally by setting the coupling term $D(k) = 0$. If $D(k) > 0$ for all k, then both branches are real-valued for all wavenumbers k, and the linearised system is spectrally stable. Here $\gamma = \nu = 0$ and $\alpha\lambda > 0$ so that $D(k) > 0$ for all k.

We also assume that $c > 0, I_1 > 0, I_2 > 0$, and so $\lambda_{1,2} > 0$, so that $\delta > 0$, and $0 < \alpha\lambda = \delta/4$. In particular the coupling coefficient $D(k) = \alpha\lambda k^4 > 0$ for all $k > 0$. Also we recall that $\Delta < 0$ without loss of generality. The main effect of the background shear is that now $\beta \neq \mu$, and indeed each can be either positive or negative. It is useful now to examine the limits $k \to 0, \infty$. Thus

$$c_{p1,p2} \to \frac{F_{1,2}}{k^2}\,, 2F_{1,2} = \beta + \mu \pm |\beta - \mu| \quad \text{as} \quad k \to 0\,, \tag{84}$$

$$c_{p1,p2} \to E_{1,2}k^2\,, 2E_{1,2} = -(1 + \delta) \pm \{(1 - \delta)^2 + 4\alpha\lambda\}^{1/2} \quad \text{as} \quad k \to \infty\,. \tag{85}$$

$$c_{g1,g2} \to -\frac{F_{1,2}}{k^2} \quad \text{as} \quad k \to 0\,, \tag{86}$$

$$c_{g1,g2} \to 3E_{1,2}k^2 \quad \text{as} \quad k \to \infty\,. \tag{87}$$

Note that since $0 < \alpha\lambda < \delta$, $E_2 < E_1 < 0$. One can see that there are four possibilities of qualitatively different behaviour of the dispersion relation, depending on the signs of the coefficients β and μ. Here, we study the normal oceanic case when the background shear is relatively weak compared to the intrinsic speeds $(g_1h_1)^{1/2}, (g_3h_3)^{1/2}$ when both coefficients are positive, $\beta > 0, \mu > 0$. Then $F_1 = \max[\beta, \mu] > F_2 = \min[\beta, \mu] > 0$. A typical dispersion relation is shown in Fig. 1. There is no spectral gap in either mode, and this case is similar to the scenario without any background shear, which we have studied in our previous paper[16], but with the important difference that now $\beta \neq \mu$ due to the effect of the background shear flow. Both group velocities are negative, and each has a turning point. For the case shown in Fig. 1, $\Delta = -0.1\,ms^{-1}, \beta = 1\,m^2s^{-2}$, $g_{1,3} = 1 \times 10^{-1}\,ms^{-2}$, $h_1 = 50\,m$, $h_3 = 100\,m$, $U_1 = 1\,m\,s^{-1}$, which yields $\alpha = -0.707, \delta = 1.414, \lambda = -0.5, \mu = 0.604\,m^2s^{-2}$.

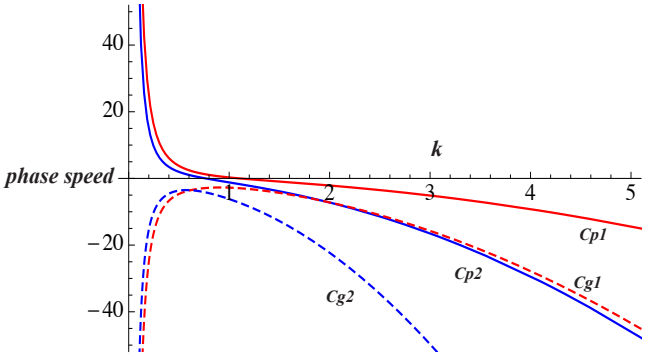

Fig. 1. Typical dispersion curve with $\alpha = -0.707\,, \delta = 1.414\,, \lambda = -0.5\,, \beta = 1\,m^2s^{-2}, \mu = 0.604\,m^2s^{-2}$, $\Delta = -0.1\,ms^{-1}$.

4. Numerical simulations

In this section we present some preliminary numerical results using the scaled equations (54, 55) for parameter settings corresponding to Fig. 1. Note that in these equations X, T are scaled variables, see (53), and have dimensions of $C^{-1/2}, C^{-3/2}$ respectively, where C is a velocity scale. The dependent variables u and v have the dimension of C. The coefficients $n, m, \alpha, \delta, p, q, \lambda$ are dimensionless, while β, γ, μ, ν have dimensions of C^2, and Δ has the dimension of C. For all examples considered in this paper we have

$$n = m = p = q = \gamma = \nu = 0$$

(see section 2.2). The numerical scheme is the same pseudo-spectral scheme as that used in our previous work[16]. The initial conditions are either an approximation to a KdV solitary wave, as described in[16], or an approximation to a nonlinear wave packet described in[10]. Both kinds were employed here, and some typical outcomes are described in this section. The former initial condition, denoted as the weak coupling KdV solitary wave, is described as follows,

$$u = a\,\mathrm{sech}^2(\sigma_1 X)\,, \quad \frac{a}{3} = 4(1+\alpha)\sigma_1^2\,, \tag{88}$$

$$v = b\,\mathrm{sech}^2(\sigma_2 X)\,, \quad \frac{b}{3} = 4(\delta+\lambda)\sigma_2^2\,. \tag{89}$$

This was implemented with the constraint of $\sigma_1 = \sigma_2$ and note that here the nonlinear terms $(u^2/2)_{XX}$, $(v^2/2)_{XX}$ have maximum absolute values of $2a^2\sigma_1^2 = a^3/6(1+\alpha)$ and $2b^2\sigma_2^2 = b^3/6(\delta+\lambda)$ respectively.

The nonlinear wave packet initial condition is here based on a maximum point in either of the group velocity curves where $\partial c_g/\partial k = 0$ and $k = k_{1,2}$ according to whether the maximum point is for mode 1 or mode 2. To obtain a suitable wave packet initial condition, the procedure is to choose $k = k_{1,2}$ and then find the ratio u_0/v_0 from (79) or (80) in the form $u_0 = U_0 a_0, v_0 = V_0 a_0$ where a_0 is an arbitrary function of X, but U_0, V_0 are known functions of k. Based on the expected outcome that the nonlinear wave packet will be governed by an evolution equation such as the nonlinear Schrödinger equation, we choose $a_0(X) = A_0\text{sech}(K_0 X)$. The underlying theory, see [10], suggests that the shape should be sech, and that K_0 depends on the amplitude A_0. Here we instead choose a value of $K_0 << k$, say $K_0 = 0.1k$ or $K = 0.2k$. Then the wave packet initial condition is

$$u(X,0) = rV_0A_0\text{sech}(K_0X)\cos(kX)\,, \quad v(X,0) = V_0A_0\text{sech}(K_0X)\cos(kX)\,, \tag{90}$$

where $r = U_0/V_0$ is a known function of k, and we can choose V_0 arbitrarily, say $V_0 = 1$.

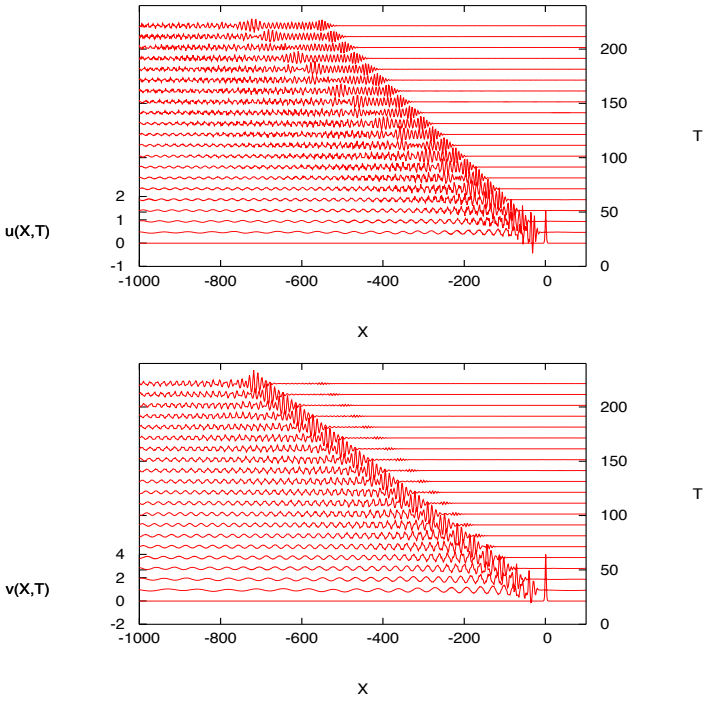

Fig. 2. Numerical simulations using a KdV solitary wave initial condition (88, 89) with $a = 1.4\,, b = 4.38$.

Using the KdV solitary wave initial conditions (88, 89) a typical numerical result is shown in Fig. 2 and Fig. 3. Two wave packets can be seen in the u-component, but one of them is too small to be seen in the v-component. However, a comparison of the numerical modal ratio u_0/v_0 shows a very good agreement with the theoretical prediction from the dispersion relation. The calculated numerical modal ratio is given by $R \approx 2.72$ for c_{g1} and $R \approx 0.27$ for c_{g2}. The speeds $-2.78, -3.58$ and the ratios of the numerically found wave packets are in agreement with the theoretical predictions. Here, the maximum group speeds from the linear dispersion relation, $c_{g1} \approx -2.72$ and $c_{g2} \approx -3.50$, while the wave numbers for each group speed indicate that $k_1 = 0.91$ and $k_2 = 0.58$.

Fig. 4 shows the numerical results initiated using the wave packet initial conditions (90) with $k = k_1 = 0.91$ and $r \approx 2.74$. We can clearly see the emergence of a nonlinear wave packet propagating to the left with the speed -2.73, which is close to the theoretical prediction of $c_{g1} = -2.72$. The additional radiation to the left is associated with a speed -3.77, which is close to the theoretical prediction of $c_{g2} = -3.50$. Fig. 5 shows the numerical results initiated using wave packet initial conditions (90) with $k = k_2 = 0.58$ without the ratio value for $v(X,0)$. Again, we

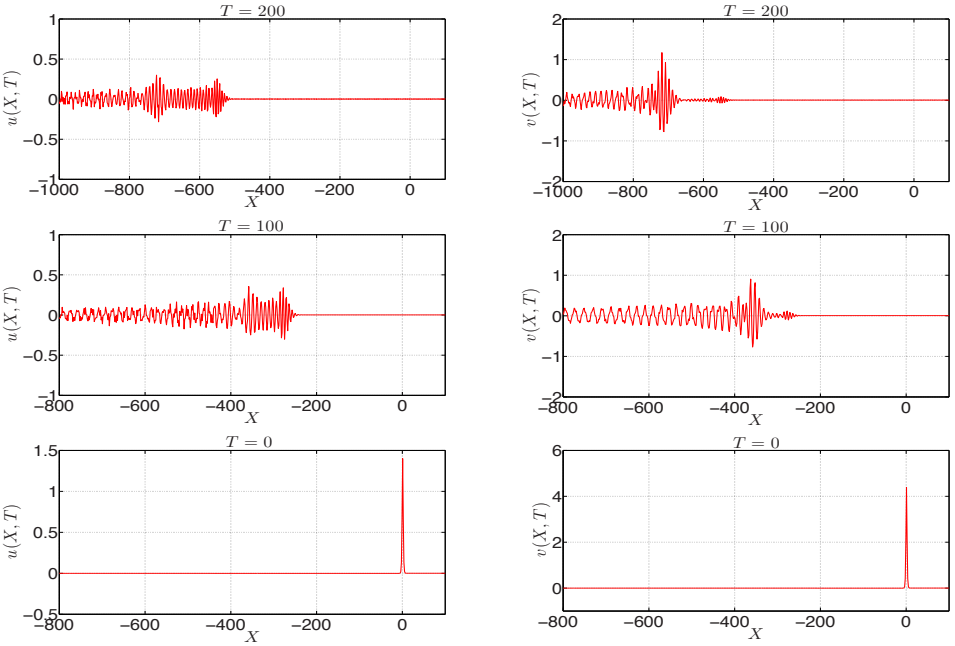

Fig. 3. Same as Fig. 2, but a cross-section at $T = 0\,, T = 100\,, T = 200$.

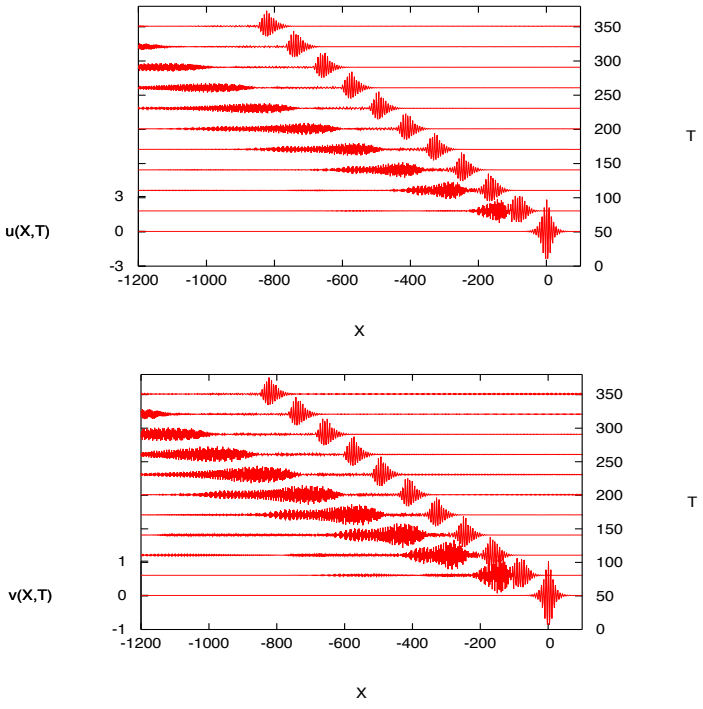

Fig. 4. Numerical simulations using a wave packet initial condition (90) with $k = k_1$ and $A_0 = 1$.

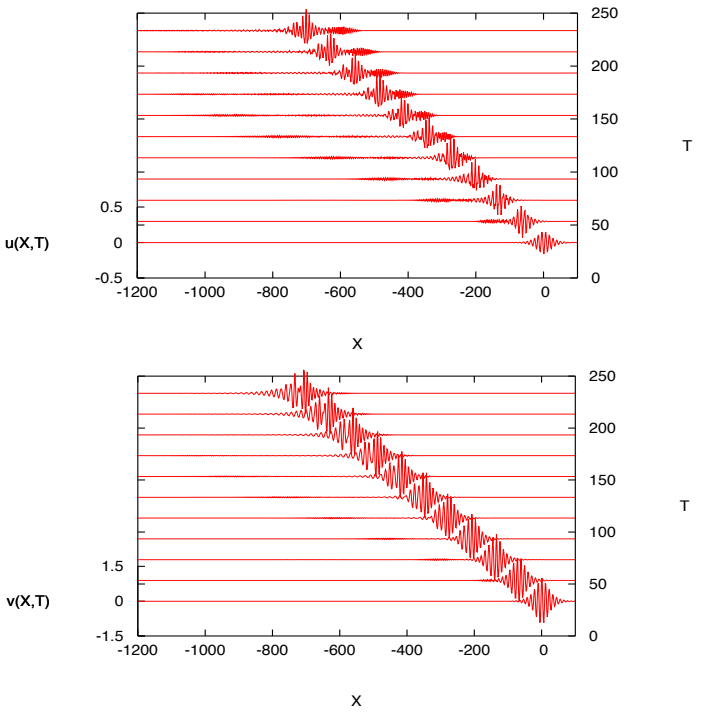

Fig. 5. Numerical simulations using a wave packet initial condition (90) with $k = k_2$ and $A_0 = 1$.

can clearly see one wave packet emerging and propagating with the speed -3.63, close to the theoretical prediction of $c_{g2} = -3.50$. Here there is also a small unsteady wave packet, seen in the u-component, moving with the speed -2.96 close to the theoretical prediction of $c_{g1} = -2.72$. Note that the scale for the u and v components are different.

5. Discussion

In this paper we have briefly reviewed in section 2.1 the derivation of coupled Ostrovsky equations for resonantly interacting weakly nonlinear long oceanic internal waves, presented in detail in our previous work [16]. The resulting system (43, 44) describes the evolution of the amplitudes of two linear long wave modes whose linear long wave phase speeds are nearly coincident. In an extension of our previous work, here we focus on the effect of a background shear flow, using a three-layer model as described in section 2.2. The essential difference that emerges is that the coefficients β, μ of the rotational terms in the coupled Ostrovsky equations (54, 55) (expressed in scaled form), are not necessarily positive or equal, as is the case in the absence of a background shear flow. In this preliminary study we present some numerical results for the case when $\beta > 0, \mu > 0$ which arises when the background shear flow is rather weak compared to the intrinsic mode speeds in the absence of the shear flow, but $\beta \neq \mu$. The linear dispersion relation, discussed in section 3, is then qualitatively similar to that presented in our previous work [16], see Fig. 1. In this case, each mode has a maximum in the group velocity at certain wave numbers k_1, k_2, and based on the study [10] for a single Ostrovsky equation (1), and on our previous work [16] for coupled Ostrovsky equations, we expect the longtime outcome to be the emergence of nonlinear wave packets based on these wavenumbers.

This hypothesis is tested numerically in section 4, using three different initial conditions. Fig. 2 and Fig. 3 show the case when the initial condition is a KdV-type solitary wave, which has no *a priori* wavenumber selection. As expected, the emergence of two nonlinear wave packets based on the wavenumbers k_1, k_2 is clearly seen, with speeds in agreement with the theoretical predictions. In contrast, Fig. 4 and Fig. 5 show the cases when the initial condition is

a wave packet based on the predicted wave numbers k_1, k_2 respectively. As expected, the emergence of the nonlinear wave packet is now more pronounced, although interestingly, in each case there is some transfer of energy to the other wavenumber, that is, an initial condition based on $k_1(k_2)$ generates not only a wave packet with that carrier wavenumber, but also a smaller wave packet based on the other allowed wavenumber $k_2(k_1)$. These are preliminary results when there is a background shear, and our future work will examine these scenarios further, and also examine the interesting cases when β, μ are not necessarily positive, a situation which cannot arise when there is no background shear flow.

Acknowledgements

A. Alias is supported by Universiti Malaysia Terengganu and the Ministry of Higher Education of Malaysia.

References

1. Grimshaw R. Internal solitary waves. In: Grimshaw R, editor. *Environmental Stratified Flows*. Boston: Kluwer; 2001. Chapter 1, p. 1-29.
2. Helfrich KR, Melville WK. Long nonlinear internal waves. *Ann. Rev. Fluid Mech.* 2006; **38:** 395-425.
3. Grimshaw RHJ, Ostrovsky LA, Shrira VI, Stepanyants YuA. Long nonlinear surface and internal gravity waves in a rotating ocean. *Surveys Geophysics* 1998; **19:** 289-338.
4. Ostrovsky L. Nonlinear internal waves in a rotating ocean. *Oceanology* 1978; **18:**119-125.
5. Grimshaw R. Evolution equations for weakly nonlinear, long internal waves in a rotating fluid. *Stud. Appl. Math.* 1985; **73:** 1-33.
6. Grimshaw, R. Models for nonlinear long internal waves in a rotating fluid. *Fundamental and Applied Hydrophysics*, 2013; **6:** 4-13.
7. Grimshaw R, Helfrich K. The effect of rotation on internal solitary waves, *IMA J. Appl. Math.* 2012; **77:** 326-339.
8. Grimshaw RHJ, He J-M, Ostrovsky LA. Terminal damping of a solitary wave due to radiation in rotational systems. *Stud. Appl. Math* 1998; **101:** 197-210.
9. Helfrich K. Decay and return of internal solitary waves with rotation. *Phys. Fluids* 2007; **19:** 026601.
10. Grimshaw R, Helfrich K. Long-time solutions of the Ostrovsky Equation. *Stud. Appl. Math* 2008; **121:** 71-88.
11. Yagi D, Kawahara T. Strongly nonlinear envelope soliton in a lattice model for periodic structure, *Wave Motion* 2001; **34:** 97-107.
12. Gerkema T. A unified model for the generation and fission of internal tides in a rotating ocean. *J. Mar. Res.* 1996; **54:** 421-450.
13. Eckart C. Internal Waves in the Ocean. *Phys. Fluids* 1961; **4:** 791-799.
14. Gear J, Grimshaw R. Weak and strong interactions between internal solitary waves. *Stud. Appl. Math.* 1984: **70:** 235-258.
15. Grimshaw R. Coupled Korteweg-de Vries equations. In: *Without Bounds: A Scientific Canvas of Nonlinearity and Complex Dynamics.*, Springer, 2013; 317-334.
16. Alias A, Grimshaw RHJ, Khusnutdinova KR. On strongly interacting internal waves in a rotating ocean and coupled Ostrovsky equations. *Chaos* 2013; **23:** 023121.
17. Khusnutdinova KR, Samsonov AM., Zakharov AS. Nonlinear layered lattice model and generalized solitary waves in layered elastic structures. *Phys. Rev. E* 2009; **79:** 056606.
18. Khusnutdinova KR, Moore KR. Initial-value problem for coupled Boussinesq equations and a hierarchy of Ostrovsky equations. *Wave Motion* 2011; **48:** 738-752.